

Multicluster accompanied fission

D. N. Poenaru,^{1,2,3,4} W. Greiner,^{2,3} J. H. Hamilton,³ A. V. Ramayya,³ E. Hourany,⁴ and R. A. Gherghescu^{1,2}

¹National Institute of Physics and Nuclear Engineering, P.O. Box MG-6, RO-76900 Bucharest, Romania

²Institut für Theoretische Physik der Universität, Postfach 111932, D-60054 Frankfurt am Main, Germany

³Department of Physics and Astronomy, Vanderbilt University, Nashville, Tennessee 37235

⁴Institut de Physique Nucléaire, F-91406 Orsay Cedex, France

(Received 18 February 1999)

In this process a heavy or superheavy nucleus spontaneously breaks into four, five, or six nuclei of which two are asymmetric or symmetric heavy fragments and the others are light clusters, e.g., α particles, ^{10}Be , ^{14}C , ^{20}O , or combinations of them. Examples are presented for the two-, three-, and four-cluster accompanied cold fission of ^{252}Cf and ^{262}Rf , in which the emitted clusters are 2α , $\alpha + ^6\text{He}$, $\alpha + ^{10}\text{Be}$, $\alpha + ^{14}\text{C}$, 3α , $\alpha + ^6\text{He} + ^{10}\text{Be}$, $2\alpha + ^6\text{He}$, $2\alpha + ^8\text{Be}$, $2\alpha + ^{14}\text{C}$, and 4α . A comparison is made with the recently observed ^{252}Cf cold binary fission, and cold ternary (accompanied by α particle or by ^{10}Be cluster). The strong shell effect corresponding to the doubly magic heavy fragment ^{132}Sn is emphasized. The most favorable mechanism of such a decay mode should be the emission from an elongated neck formed between the two heavy fragments. [S0556-2813(99)03906-0]

PACS number(s): 25.85.Ca, 23.90.+w, 23.70.+j

Neutron multiplicities higher than one have been observed since the early times of nuclear fission investigation. Once the condition of a positive released energy, $Q > 0$, is fulfilled, the escape of one or several neutrons from the neck formed between the light and heavy fragment, is not prevented by any Coulomb force. A small and narrow centrifugal barrier, due to the angular momenta carried away by the neutrons, does not constitute a major obstacle.

A charged particle has to penetrate, by quantum tunneling, a much thicker and higher potential barrier, leading to a long delay and to a corresponding comparable low yield. Nevertheless, the particle-accompanied fission (or ternary fission) was observed both in neutron-induced and spontaneous fission. It was discovered in 1946 [1,2]. Several such processes, in which the charged particle is a proton, deuteron, triton, $^3\text{-}^8\text{He}$, $^6\text{-}^{11}\text{Li}$, $^7\text{-}^{14}\text{Be}$, $^{10}\text{-}^{17}\text{B}$, $^{13}\text{-}^{20}\text{C}$, $^{15}\text{-}^{20}\text{N}$, $^{15}\text{-}^{22}\text{O}$, have been detected. Many other heavier isotopes of F, Ne, Na, Mg, Al, Si, P, S, Cl, Ar, and even Ca were recently mentioned [3]. This rare process is different from cluster radioactivity [4,5], which can be considered a binary superasymmetric cold fission phenomenon. The cluster emitted in a binary process has a well defined energy (the kinetic energy $E_k = QA_d/A$, where A_d and A are the mass numbers of the daughter and parent nuclei, respectively), while in a ternary one the energy spectrum is very broad, extends to much higher limit and possesses a much higher most probable value. In a cold fission process [6] the fragments are neither excited nor strongly deformed, hence no neutron is evaporated from excited fragments or from the compound nucleus; the total kinetic energy of the fragments exhausts the released energy. In more complex than binary phenomena (ternary, quaternary, etc), neutrons could still be emitted from the neck, because the Q value is positive. In this case their kinetic energy added to those of the fragments should exhaust the total released energy. Two or even three clusters emitted from the same parent have been detected [7] in cluster radioactivity. They are, like in binary fission, alternative ways of splitting, and not simultaneous emission of several particles.

Forty years ago [8] it was shown, on the basis of the liquid drop model, that for increasingly heavier nuclei, fission into three, then four, and even five fragments becomes energetically more favorable than binary fission. Swiatecki took into consideration only equally sized fragments and ignored any shell effect. The “true” (in which the fragments are equally sized) ternary or quaternary spontaneous cold fission has not been experimentally discovered until now. On the other side the multifragmentation process taking place at high excitation energies, well over the potential barrier, is intensively studied [9].

A very powerful technique, based on the fragment identification by using $\gamma\text{-}\gamma\text{-}\gamma$ coincidences in the multiple Ge-detector Compact Ball facility at Oak Ridge National Laboratory, and more recently in the GAMMASPHERE with 72 Ge Compton-suppressed detectors, was developed and employed to discover new characteristics of the fission process [10,11], and new decay modes (emission of an alpha particle and of ^{10}Be [12], accompanying the cold fission of ^{252}Cf , the double fine structure, and the triple fine structure in binary and ternary fission, respectively). This technique will be hopefully extended in the future to more complex phenomena, including the nuclear division into more than three fragments.

We start by a brief sketch of the calculations, and then we discuss some typical results, presented in Figs. 1–3. The basic condition to be fulfilled in a spontaneous emission process of high complexity, $^AZ \rightarrow \sum_1^n A_i Z_i$, concerns the released energy (Q value)

$$Q = M - \sum_1^n m_i, \quad (1)$$

which should be positive and high enough in order to assure a relatively low potential barrier height. We took the masses (in units of energy), entering in the above equation, from the most recently updated compilation of measurements [13]. When the number $n=2$ one has a binary process, $n=3$

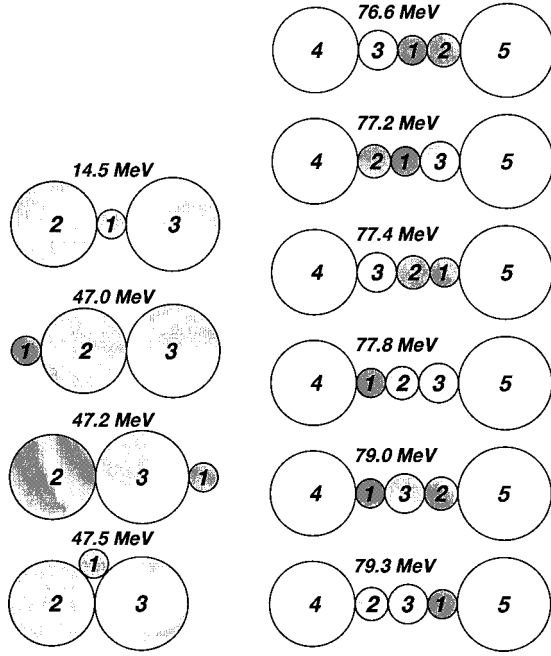


FIG. 1. Aligned and compact configurations for α accompanied cold fission of ^{252}Cf with doubly magic ^{132}Sn heavy fragment (left-hand side), and aligned configurations with three clusters between the light and heavy fragment for $\alpha + {}^6\text{He} + {}^{10}\text{Be}$ accompanied cold fission of ^{252}Cf with ^{132}Sn heavy fragment (right-hand side). The corresponding energies are shown.

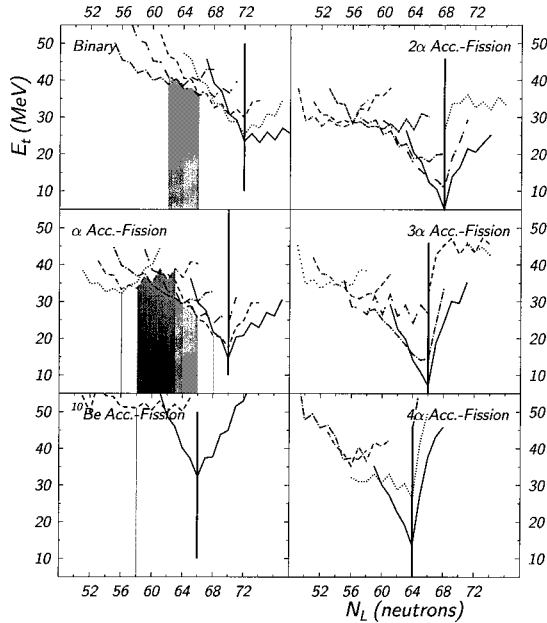


FIG. 2. The energy of the optimum aligned configurations of fragments in contact for the cold fission of ^{252}Cf versus the neutron number of the light fragment. The experimentally determined cold binary fission, α -, and ${}^{10}\text{Be}$ accompanied fission are plotted on the left-hand side (the identified pairs are emphasized). Calculations for the 2α , 3α , and 4α accompanied fission new decay modes are given on the right-hand side. The vertical heavy bar on each graph corresponds to a magic neutron number of the heavy fragment $N_H = 82$.

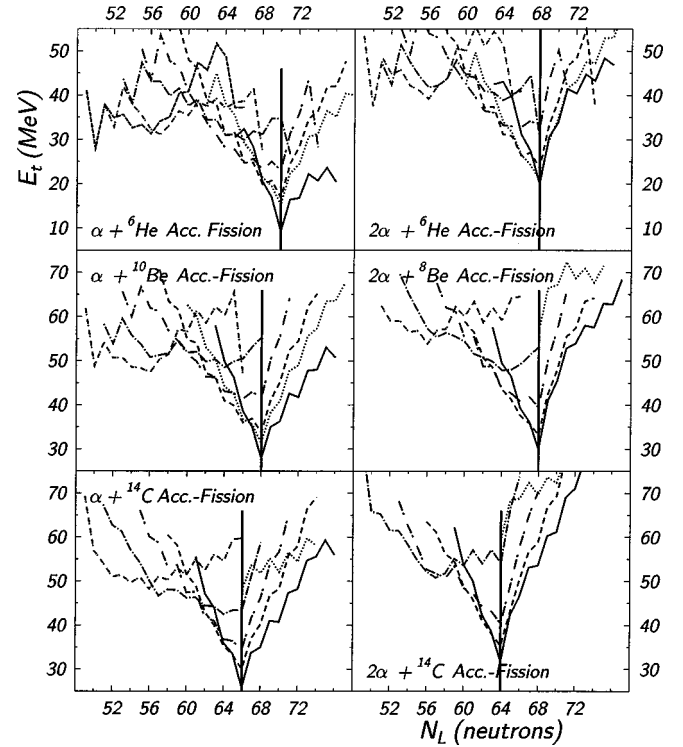


FIG. 3. On the left-hand side: the energy of the optimum aligned configurations of fragments in contact for three examples of two cluster ($\alpha + {}^6\text{He}$, $\alpha + {}^{10}\text{Be}$, and $\alpha + {}^{14}\text{C}$) accompanied cold fission of ^{262}Rf versus the neutron number of the light fragment. Calculations for the three cluster (2α plus: ${}^6\text{He}$, ${}^8\text{Be}$, and ${}^{14}\text{C}$) accompanied fission are given on the right-hand side. The vertical heavy bar on each graph corresponds to a magic neutron number of the heavy fragment $N_H = 82$.

means a ternary fragmentation, $n=4$ —a quaternary fission, $n=5$ —a division into five fragments, $n=6$ —a division into six fragments, etc. We make the following convention: $A_1 \leq A_2 \leq A_3 \leq A_4 \leq A_5 \dots \leq A_n$, e.g., for the $\alpha + {}^{10}\text{Be}$ accompanied fission of ^{252}Cf with ^{132}Sn and ${}^{110}\text{Ru}$ fragments $A_1 = 4$, $A_2 = 10$, $A_3 = 110$, and $A_4 = 132$. This convention will help us to label the different modes of ordering the fragments when they are lying on the same axis.

In a first approximation, one can obtain an order of magnitude of the potential barrier height by assuming spherical shapes of all the participant nuclei. This assumption is realistic if the fragments are magic nuclei. For deformed fragments it leads to an overestimation of the barrier. By taking into account the prolate deformations, one can get smaller potential barrier height, hence better condition for multicluster emission. We use the Yukawa-plus-exponential (Y+E) double folded model [14] extended by us for different charge densities. In the decay process from one parent to several fragments, the nucleus deforms, reaches the touching configuration, and finally the fragments become completely separated. A phenomenological shell and pairing correction energy is introduced by subtracting the “partial” Q_{ij} value from each component of the interaction energy, E_{ij} , at the touching configuration

$$E_t = \sum_i^n \sum_{j>i}^n (E_{ij} - Q_{ij}); \quad E_{ij} = E_{Cij} + E_{Yij}, \quad (2)$$

where E_{ij} ($i, j = 1, 2, \dots, n$) is the sum of the Coulomb and Y+E potential energies, given below for spherical shapes. For calculation of both E_{ij} and Q_{ij} we consider a ‘‘partial’’ compound nucleus with a mass number $A_{ij} = A_i + A_j$, and an atomic number $Z_{ij} = Z_i + Z_j$. The origin of the potential energy is taken at an infinite separation distance of the fragments. In such a way one has initially, for the undeformed parent, a potential energy equal to the Q value, motivating our procedure.

By assuming a uniform distribution of the electric charge, the electrostatic interaction energy of nonoverlapping spherical nuclei $A_i Z_i$ and $A_j Z_j$ is the same as if the charges were concentrated at the sphere centers. Consequently one has

$$E_{Cij} = e^2 Z_i Z_j / R_{ij}, \quad (3)$$

where R_{ij} is the distance between centers, which becomes $R_{ij} = r_0(A_i^{1/3} + A_j^{1/3})$ at the touching point. Within the Myers-Swiatecki’s liquid drop model (LDM) there is no contribution of the surface energy to the interaction of the separated fragments; the barrier has a maximum at the touching point configuration. The proximity forces acting at small separation distances (within the range of strong interactions) give rise in the Y+EM to a term expressed as follows:

$$E_{Yij} = -4 \left(\frac{a}{r_0} \right)^2 \sqrt{a_{2i} a_{2j}} \left[g_i g_j \left(4 + \frac{R_{ij}}{a} \right) - g_i f_i - g_j f_j \right] \frac{\exp(-R_{ij}/a)}{R_{ij}/a}, \quad (4)$$

where

$$g_k = \frac{R_k}{a} \cosh\left(\frac{R_k}{a}\right) - \sinh\left(\frac{R_k}{a}\right), \quad (5)$$

$$f_k = \left(\frac{R_k}{a} \right)^2 \sinh\left(\frac{R_k}{a}\right), \quad (6)$$

in which R_k is the radius of the nucleus $A_k Z_k$, $a = 0.68$ is the diffusivity parameter, and a_{2i}, a_{2j} are expressed in terms of the model constants a_s, κ and the nuclear composition parameters I_i and I_j , $a_2 = a_s(1 - \kappa I^2)$, $a_s = 21.13$ MeV, $\kappa = 2.3$, $I = (N - Z)/A$, $R_0 = r_0 A^{1/3}$, $r_0 = 1.16$ fm is the radius constant, and e is the electron charge, $e^2 \approx 1.44$ MeV fm.

By performing extensive calculations [15] we have seen a clear correlation between the Q values and the measured yield of different isotopes for one cluster accompanied fission. For example, among the He isotopes with mass numbers 4, 6, and 8, ${}^4\text{He}$ leads to the maximum Q value; the maximum yield was indeed experimentally observed [2] for α accompanied fission. Similarly, among ${}^{6,8,10,12}\text{Be}$, the clusters ${}^8\text{Be}$ and ${}^{10}\text{Be}$ give the maximum Q values.

As ${}^8\text{Be}$ spontaneously breaks into 2α particles it is not easy to measure ${}^8\text{Be}$ accompanied fission yield; consequently ${}^{10}\text{Be}$ has been most frequently identified. By detecting, in coincidence, two alpha particles flying from the neck on the same axis in opposite directions, the ${}^8\text{Be}$ accompanied fission with a larger yield compared to that of the ${}^{10}\text{Be}$ one, could be observed in the future.

From ${}^{12,14,16,18}\text{C}$ the favoured is ${}^{14}\text{C}$, and all ${}^{16,18,20,22}\text{O}$ isotopes have comparable Q values when they are emitted in a cold binary fission of ${}^{252}\text{Cf}$. Nevertheless, ${}^{20}\text{O}$ is slightly higher than the others. As a rule, if the Q value is larger the barrier height is smaller, and the quantum tunneling becomes more probable.

On the left-hand side of Fig. 1 we show different kinds of aligned configurations of fragments in contact and we compare the corresponding energies. There are three aligned fragments on the same axis, in the following order of the three partners: 213, 123, and 132 (or 231) and of the compact configuration (in which every partner is in touch with all others). It is clear that the potential barrier for the ‘‘polar emission’’ (123 or 132) is much higher than that of the emission from the neck (213), which explains the experimentally determined low yield of the polar emission compared to the ‘‘equatorial’’ one. As it should be, the compact configuration possesses the maximum total interaction energy, hence it has the lowest chance to be observed. An important conclusion can be drawn, by generalizing this result, namely: *the multiple clusters 1,2,3, . . . should be formed in a configuration of the nuclear system in which there is a relatively long neck between the light ($n-1$) and heavy (n) fragment*. Such shapes with long necks in fission have been considered [16], as early as 1958.

On the right-hand side of Fig. 1, we ignore the aligned configurations in which the heavy fragments are not lying at the two ends of the chain. By arranging in six different manners the α -particle, ${}^6\text{He}$, and ${}^{10}\text{Be}$ clusters between the two heavy fragments from the cold fission of ${}^{252}\text{Cf}$, the difference in energy is relatively small. Nevertheless, the 43125 configuration seems to give the lowest barrier height.

On the left-hand side of Fig. 2 we plotted the energies at the touching point configurations for the known binary and ternary cold fission decay modes of ${}^{252}\text{Cf}$. On the right-hand side there are new decay modes which have a good chance to be detected: 2α , 3α , and 4α accompanied fission. In order to emphasize the strong shell effect, we have chosen in the abscissa the number of neutrons of the light fragment, N_L , which in turn corresponds to a well defined neutron number of the heavy fragment, N_H , for a given parent and a given cluster accompanied fission, in our case to $N_H = 150 - N_L$ for 2α accompanied fission, $N_H = 148 - N_L$ for 3α accompanied fission, and $N_H = 146 - N_L$ for 4α accompanied fission. The vertical heavy bar on each plot helps to determine the position of the magic number $N_H = 82$. Different types of lines are drawn through the points belonging to the same combination of atomic numbers of the fragments $Z_L - Z_H$. The full line is always reserved for the pair in which the heavy fragment is an isotope of Sn (with $Z_H = 50$ magic number). We have only plotted the results for even Z_L and Z_H , because they can be identified more easily by using the technique of triple- γ coincidences. The conclusion is clear: the minimum barrier height is always obtained when the heavy fragment is the doubly magic ${}^{132}\text{Sn}$. The investigated pairs are emphasized. These are for the binary fission [10,11] (at the top): ${}_{40}^{102,104}\text{Zr} - {}_{58}^{150,148}\text{Ce}$ ($N_L = 62, 64$), ${}_{42}^{104-108}\text{Mo} - {}_{56}^{148-144}\text{Ba}$ ($N_L = 62 - 66$), ${}_{44}^{110}\text{Ru} - {}_{54}^{142}\text{Xe}$ ($N_L = 66$), and ${}_{46}^{116}\text{Pd} - {}_{52}^{136}\text{Te}$ ($N_L = 70$). For cold α accompanied fission [12] (in the intermediate part): ${}_{36}^{92}\text{Kr} - {}_{60}^{156}\text{Nd}$ ($N_L = 56$), ${}_{38}^{96-101}\text{Sr} - {}_{58}^{152-147}\text{Ce}$

($N_L = 58 - 63$), $^{100-104}_{40}\text{Zr}-^{148-144}_{56}\text{Ba}$ ($N_L = 60 - 64$), $^{106-108}_{42}\text{Mo}-^{142-140}_{54}\text{Xe}$ ($N_L = 64 - 66$), $^{112}_{44}\text{Ru}-^{136}_{52}\text{Te}$ ($N_L = 68$), and $^{116}_{46}\text{Pd}-^{132}_{50}\text{Sn}$ ($N_L = 70$). At the bottom, there is one example of detected cold ^{10}Be accompanied fission of ^{252}Cf , namely $^{96}_{38}\text{Sr}-^{146}_{56}\text{Ba}$ ($N_L = 58$) [12].

The energies of the optimum configuration of fragments in contact, in the right-hand side of Fig. 2 and in Fig. 3, are not much higher than what has been already measured, which looks very promising for the possibility of detecting the 2α , 3α , and 4α accompanied fission decay modes. By taking into account the mass values of the participants, one can see that the Q value for the 2α accompanied fission may be obtained by translation with $+0.091$ MeV from the Q value of the ^{10}Be accompanied fission. A similar translation with -7.275 MeV should be made from the ^{12}C accompanied fission in order to obtain the Q values of the 3α accompanied fission, etc.

When the parent nucleus is heavier, the multicuster emission is stronger. We perform calculations for heavier parent nuclei: $^{252,254}\text{Es}$, $^{255,256}\text{Fm}$, $^{258,260}\text{Md}$, $^{254,256}\text{No}$, ^{262}Lr , $^{261,262}\text{Rf}$, etc. Some results, for multicuster ($\alpha + ^6\text{He}$, $\alpha + ^{10}\text{Be}$, $\alpha + ^{14}\text{C}$, $2\alpha + ^6\text{He}$, $2\alpha + ^8\text{Be}$, and $2\alpha + ^{14}\text{C}$) emission from ^{262}Rf , are presented in Fig. 3.

While the minimum energy of the most favorable aligned configuration of fragments in contact, when at least one cluster is not an alpha particle, becomes higher and higher with increasing complexity of the partners, the same quantity for multi-alphas remains favorable, hence we expect that multi-alpha emission could be more easily experimentally detected.

This work was supported by Bundesministerium für Bildung und Forschung (BMBF), Bonn; Deutsche Forschungsgemeinschaft (DFG), Gesellschaft für Schwerionenforschung (GSI), Darmstadt; Graduirtenkolleg Schwerionenphysik, Deutscher Akademischer Austauschdienst (DAAD). The work at Vanderbilt University was supported in part by the U.S. Department of Energy under Contract No. DE-FG05-88ER40407 and the Joint Institute for Heavy Ion Research is supported by its members, University of Tennessee, Vanderbilt University, and the U.S. Department of Energy through Contract No. DE-FG05-87ER40311 with the University of Tennessee, Institut de Physique Nucléaire, Orsay, and Ministry of Research and Technology, Bucharest. One of us (D.N.P.) would like to acknowledge the hospitality and financial support received during his research stage in Frankfurt am Main, Nashville, and Orsay, when the present work was completed.

-
- [1] T. San-Tsiang *et al.*, R. Chastel, H. Zah-Way, and L. Vigneron, C. R. Hebd. Seances Acad. Sci. **223**, 986 (1946).
- [2] M. Mutterer and J.P. Theobald, *Nuclear Decay Modes* (IOP, Bristol, 1996), p. 487.
- [3] F. Gönnenwein *et al.*, Nuovo Cimento A **110**, 1089 (1997).
- [4] A. Sandulescu, D.N. Poenaru, and W. Greiner, Fiz. Elem. Chastits At. Yadra **11**, 1334 (1980) [Sov. J. Part. Nucl. **11**, 528 (1980)].
- [5] D.N. Poenaru and W. Greiner, *Nuclear Decay Modes* (Ref. [2]), p. 275.
- [6] C. Signarbieux *et al.*, J. Phys. (France) Lett. **42**, L437 (1981).
- [7] P.B. Price and S.W. Barwick, *Particle Emission from Nuclei*, Vol. II (CRC, Boca Raton, 1989), p. 205.
- [8] W.J. Swiatecki, *Proceedings of the 2nd UN International Conference on the Peaceful Uses of Atomic Energy* (United Nations, Geneva, 1958), p. 248.
- [9] L.G. Moretto *et al.*, Phys. Rev. Lett. **77**, 2634 (1996).
- [10] J.H. Hamilton *et al.*, J. Phys. G **20**, L85 (1994).
- [11] G.M. Ter-Akopian *et al.*, Phys. Rev. Lett. **77**, 32 (1996).
- [12] A.V. Ramayya *et al.*, Phys. Rev. C **57**, 2370 (1998); Phys. Rev. Lett. **81**, 947 (1998).
- [13] G. Audi and A.H. Wapstra, Nucl. Phys. A **595**, 409 (1995).
- [14] H.J. Krappe, J.R. Nix, and A.J. Sierk, Phys. Rev. C **20**, 992 (1979).
- [15] D.N. Poenaru, W. Greiner, and R.A. Gherghescu, At. Data Nucl. Data Tables **68**, 91 (1998).
- [16] D.L. Hill, in *Proceedings of the 2nd UN International Conference on the Peaceful Uses of Atomic Energy*, Ref. [8], see also Ref. [11], p. 244, therein.